Interactions of T7 RNA Polymerase with T7 Late Promoters Measured by Footprinting with Methidiumpropyl-EDTA–Iron(II)†

Samuel I. Gunderson,* Kenneth A. Chapman,‡ and Richard R. Burgess
McArdle Laboratory for Cancer Research and Laboratory of Genetics, University of Wisconsin, Madison, Wisconsin 53706
Received September 23, 1986; Revised Manuscript Received November 19, 1986

ABSTRACT: The interactions of T7 RNA polymerase with T7 late promoters were studied by using quantitative footprinting with methidiumpropyl-EDTA·Fe(II) [MPE-Fe(II)] as the DNA cleaving agent. Class II and class III T7 promoters have a highly conserved 23 base pair sequence from −17 to +6. Among class III promoters the −22 to −18 region is also highly conserved. For a class II promoter, T7 RNA polymerase protects the −17 to −4 region from MPE-Fe(II) cleavage; when GTP is present, protection extends from −17 to +5 (noncoding strand). For a class III promoter, protection extends from −20 to −4 and in the presence of GTP from −20 to +5 (noncoding strand). The protected regions for the coding strands of both promoters were nearly identical with that seen for the noncoding strands. The binding constant for the class III promoter is $(4 \pm 1.5) \times 10^7$ M^{-1} and in the presence of GTP increases to $(10 \pm 1.7) \times 10^7$ M^{-1}. These binding constants are about 1000 and 200 times greater, respectively, than values reported previously [Ikeda, R. A., & Richardson, C. C. (1986) *Proc. Natl. Acad. Sci. U.S.A. 83*, 3614–3618]. The differences in binding constants are probably due to tRNA and high salt used in those earlier experiments. Both tRNA and high salt (>50 mM NaCl and >10 mM $MgCl_2$) inhibit the binding of the polymerase to the promoter. Optimal binding conditions occur at 2–5 mM $MgCl_2$ and 0–10 mM NaCl. Finally, the binding constant between T7 RNA polymerase and nonpromoter DNA sites was determined to be $(2.1 \pm 1.1) \times 10^4$ M^{-1}.

Early in the infection of *Escherichia coli* by bacteriophage T7, a new phage-encoded RNA polymerase transcribes the middle and late T7 genes from the class II and class III promoters, respectively (McAllister et al., 1981; Studier & Rosenberg, 1981). These promoters have several features that distinguish them from bacterial promoters.

One such feature is the extensive homology between the promoters, as seen in Figure 1 (Dunn & Studier, 1983). Most striking is the 23 base pair perfect match between the five class III promoters and the consensus sequence. For class II promoters the −17 to +6 region shows extensive homology with the consensus sequence. In the +3 to +6 region for class II promoters, 87% of the bases are purines but only 45% of the bases match the consensus sequence. In the −17 to +2 region of the class II promoters, there is greater than 90% homology to the consensus sequence. However, within the −22 to −18 region, class II promoters show no homology to the consensus sequence, whereas class III promoters show 84% homology to the consensus sequence. One of the goals of this paper is to characterize which bases in the −22 to +6 region are necessary for interacting with T7 RNA polymerase.

Another difference between T7 and bacterial promoters is that T7 promoter sequences are unusually long and uninterrupted. The length probably ensures that T7 promoters do not occur randomly in the bacterial host genome. Yet even including this requirement, T7 promoters still appear to be too long. This notion is supported by a recent statistical analysis that concludes that T7 promoters are overspecified (Schneider et al., 1986).

T7 RNA polymerase also differs considerably from bacterial RNA polymerases. T7 RNA polymerase consists of a single subunit with a M_r of 98 000 while bacterial RNA polymerases consist of at least five subunits with a total molecular weight of about 500 000 (Burgess, 1969; Chamberlin et al., 1970). Also, unlike bacterial RNA polymerases, T7 RNA polymerase does not require any other protein factors for accurate initiation of transcription in vitro.

This paper describes a study of the interactions between T7 RNA polymerase and T7 late promoters using quantitative footprinting methods. Footprinting is useful for determining the base pairs contacted by the polymerase and for determining a binding constant between the polymerase and promoter (Galas & Schmitz, 1978). Methidiumpropyl-EDTA·Fe(II) [MPE-Fe(II)][1] was used as the DNA cleaving agent. MPE-Fe(II) affords high resolution of the boundaries of the protected region because it cleaves DNA with little sequence specificity and because it is a relatively small molecule (Hertzberg & Dervan, 1984). Earlier investigators found the presence of GTP to be essential to detect a footprint (Basu & Maitra, 1986). However, we find that footprints can be obtained without the use of nucleotides by lowering the concentration of salt and tRNA in the reaction. Surprisingly, the binding of T7 RNA polymerase to the late promoters is stoichiometrically inhibited by tRNA. An equal concentration of nonspecific DNA base pairs does not inhibit the binding, implying that the secondary structure of tRNA is interfering with the polymerase–promoter interaction.

To optimize the binding reaction, the concentrations of $MgCl_2$, NaCl, tRNA, glycerol, and several inhibitory agents

† This work was supported in part by National Institutes of Health Grants CA07175 and CA23076. S.I.G. is supported by National Institutes of Health Genetics Predoctoral Training Grant 5 T32 GM07133 and by a grant from the Lucille P. Markey Charitable Trust, Miami, FL.
* Address correspondence to this author.
‡ Present address: MSU-DOE Plant Research Laboratory, Michigan State University, East Lansing, MI 48824.

[1] Abbreviations: MPE-Fe(II), methidiumpropyl-EDTA·Fe(II); K_{RP}, binding constant between RNA polymerase and promoter site; K_{RD}, nonspecific binding constant between RNA polymerase and nonpromoter DNA site; [RP], concentration of RNA polymerase–promoter complexes; [RD], concentration of RNA polymerase–nonpromoter DNA complexes; $[R]_T$, concentration of total RNA polymerase; $[R]_f$, concentration of free RNA polymerase; $[P]_f$, concentration of free promoters; [D], concentration of nonpromoter sites (or nucleotides); ESR, equilibrium selectivity ratio; SDS–PAGE, sodium dodecyl sulfate–polyacrylamide gel electrophoresis; EDTA, ethylenediaminetetraacetic acid; Tris-HCl, tris(hydroxymethyl)aminomethane hydrochloride.

0006-2960/87/0426-1539$01.50/0

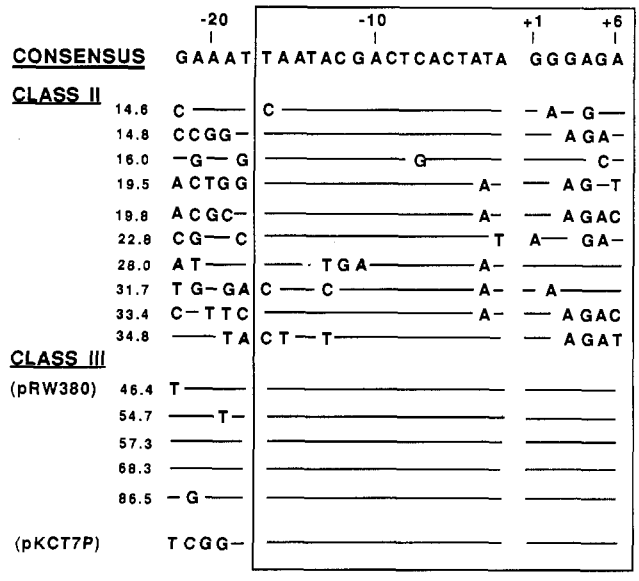

FIGURE 1: Class II and class III promoters for T7 RNA polymerase. The positions of the promoters, in T7 units, are shown to the left of the sequences. Only the bases deviating from the consensus sequence are identified, while the bases homologous to the consensus are represented as a line. Also shown are the promoters from the plasmids pKCT7P and pRW380, which are analyzed in this paper. The highly conserved 23 base pair sequence is boxed. The +3 to +6 region of the class II promoters is purine rich but deviates from the consensus sequence in 55% of the positions. The −22 to −18 region is not conserved in class II promoters but is highly conserved in class III promoters.

were varied. Binding constants were determined both in the presence and in the absence of GTP. For a class III promoter, the binding constant in the absence of GTP was found to be $(4 \pm 1.5) \times 10^7\ M^{-1}$ and in the presence of GTP increased to $(10 \pm 1.7) \times 10^7\ M^{-1}$. These two binding constants are 1000 and 200 times greater, respectively, than values previously reported (Ikeda & Richardson, 1986). The differences in binding constants are probably due to the presence of higher salt and tRNA in those earlier experiments.

As shown in Figure 1, class III promoters show sequence conservation in the −22 to −18 region while class II promoters do not. We demonstrate that T7 RNA polymerase interacts with the −22 to −18 region for class III promoters but that the footprint does not cover this region for a class II promoter. Interestingly, both promoters have almost identical binding constants (in the absence of GTP) suggesting that this region is not contributing to the overall thermodynamic stability of the complex under the conditions used. However in the presence of GTP, the binding constant for the class III promoter is nearly 3 times greater than that of the class II promoter. This implies that the −22 to −18 region is stabilizing the polymerase–promoter complex in the presence of GTP.

Materials and Methods

Plasmid Constructions. The promoter sequences of the two plasmids used in this paper are shown in Figure 1. pRW380 contains the 46.4% class III promoter cloned into the *Bam*H1 site of pBR322 (Chapman & Wells, 1982). pKCT7P contains a hybrid class II/class III promoter cloned into the *Eco*RI/*Hin*dIII site of pKO1 (unpublished results). The −22 to −18 region of the hybrid promoter is from the 14.8% class II promoter while the −17 to +6 region is from the 46.4% class III promoter.

Enzymes. T7 RNA polymerase was purified from the overproducing strain containing the plasmid pAR1219 kindly provided by F. W. Studier (Davanloo et al., 1984). The purification was a variation of the procedure of Tabor and Richardson (unpublished results; Tabor & Richardson, 1985). The final concentration of polymerase was 30 000 units/mL with a specific activity of 250 000 units/mg. The purity of the polymerase was determined to be >95% as seen by SDS–PAGE with the protein bands visualized by silver staining. Enzymes for labeling the DNA were obtained from New England Biolabs and Boehringer Mannheim Biochemicals.

Chemicals. Methidiumpropyl-EDTA (MPE) was graciously provided by Dr. Peter B. Dervan of the California Institute of Technology (Hertzberg & Dervan, 1982). $Fe(NH_4)_2(SO_4)_2 \cdot 6H_2O$ was purchased from Baker and Adamson. MPE-Fe(II) was formed by incubating equal volumes of 1 mM solutions of MPE and $Fe(NH_4)_2(SO_4)_2 \cdot 6H_2O$ at room temperature for 5 min (Hertzberg & Dervan, 1984). The MPE-Fe(II) solution was diluted appropriately and stored on ice until needed. Solutions of MPE-Fe(II) and $Fe(NH_4)_2(SO_4)_2 \cdot 6H_2O$ were always freshly prepared. [γ-^{32}P]ATP was purchased from New England Nuclear. Yeast tRNA (grade VI) from Sigma was further purified by extraction 3 times with buffer-equilibrated phenol, once with chloroform, and twice with ether and then ethanol precipitated twice followed by treatment with diethyl pyrocarbonate (DEPC). Ultrapure GTP was purchased from Pharmacia Biotechnology Group. NENSORB Sephadex columns were purchased from Du Pont.

Purification of End-Labeled DNA Fragments. End-labeled DNA fragments were prepared by a variation of the procedure of Maxam and Gilbert (1980). Plasmid DNA was digested with the primary restriction enzyme. If necessary, any blunt or 3′ overhanging ends were chewed back with DNA polymerase 1 in the presence of the appropriate deoxynucleoside triphosphate (Kornberg, 1980). The digested DNA was treated with calf intestinal alkaline phosphatase at 55 °C followed by end-labeling with T4 kinase and [γ-^{32}P]ATP. A second restriction enzyme digest was done to remove one of the labeled ends. The labeled fragments were separated by nondenaturing PAGE, and after electrophoresis the desired fragments were cut out of the gel and electroeluted. The fragments were concentrated and desalted on a prepackaged, disposable Sephadex column (NENSORB), according to the manufacturer's protocol. Prior to elution, the bound DNA fragments were washed with water to remove salt. Then the fragments were eluted from the column in 50% methanol in water, dried down, and resuspended and stored in 30% ethanol in water at −20 °C. The NENSORB column procedure had the dual advantage of removing the salt and recovering the DNA fragments without the need for addition of tRNA. Both salt and tRNA are commonly used to increase the efficiency of ethanol precipitation during fragment purification. Their elimination was critical to obtain footprints at low concentrations of T7 RNA polymerase.

The restriction enzymes used in the end-labeling procedure are described below. A 295 base pair *Dde*1/*Eco*RV fragment labeled on the coding strand at the *Dde*1 site and a 205 base pair *Sna*B1/*Dde*1 fragment labeled on the noncoding strand at the *Sna*B1 site were prepared from pKCT7P. A 317 base pair *Nae*1/*Eco*RV fragment labeled on the coding strand at the *Nae*1 site and a 225 base pair *Bsp*1/*Eco*RV fragment labeled on the noncoding strand at the *Bsp*1 site were prepared from pRW380.

Binding and Cleavage Reactions. The standard footprinting reaction (45 μL) contained 10 mM Tris-HCl, pH 7.4, 10 mM NaCl, 2 mM $MgCl_2$, and 1–10 ng of end-labeled DNA restriction fragment; 1 mM sodium ascorbate and 4 mM dithiothreitol were present as catalysts to maintain MPE-Fe(II)

in a reduced (chemically active) form. The addition of T7 RNA polymerase (or polymerase storage buffer) introduced 8 μM EDTA, 80 μM NaN_3, and 4% glycerol into the reaction. When 0.4 mM GTP was used, the $MgCl_2$ concentration was increased to 5 mM. Specific variations on the standard conditions are listed in each figure.

The footprinting reaction was started by preincubating T7 RNA polymerase with the labeled DNA (and tRNA or any nonpromoter-bearing DNA) in the standard reaction buffer (plus catalysts) for 6 min at 37 °C. Then 5 μL of 30 μM MPE-Fe(II) was added to make a final volume of 50 μL. After 6 min of cleavage at 37 °C, the reaction was stopped by the addition of 15 μl of tRNA (10 μg) in 80 mM EDTA, 10 μL of 3 M sodium acetate, and 200 μL of ethanol. The reaction was immediately chilled in liquid N_2 and the DNA was pelleted by centrifugation. The DNA was washed with 70% ethanol in water, dried, and resuspended in 90% formamide loading buffer. The samples were electrophoresed into a denaturing 8% polyacrylamide gel (Maxam & Gilbert, 1980) and the cleavage products visualized by autoradiography. Several autoradiograms were made to ensure that the exposures were within the linear response for the XAR5 emulsion. The absorbances of the autoradiographic bands were measured on a Biomed Instruments scanning densitometer (Biomed Instruments, Inc., Chicago, IL). The peak intensities were analyzed by a Macintosh Plus and the Applesoft EXCEL program.

Results

Determination of the Protected Sequence for the Promoter from pKCT7P. To investigate which bases are contacted by T7 RNA polymerase, the technique of footprinting was used to determine the region protected from MPE-Fe(II) cleavage. The first footprints were obtained by lowering the ionic strength of the reaction and by eliminating tRNA (tRNA is typically part of the purification of the labeled DNA fragment). Figure 2A is an autoradiogram of the footprinting pattern seen with increasing concentrations of T7 RNA polymerase (lanes 3–7). Specific reaction conditions are given in the figure legend.

To determine which bases are protected, densitometry of the autoradiogram was done as shown in Figure 2B. The promoter sequence was aligned with the absorbance peaks of the densitometry scan by using the marker lanes. A *Hin*fI-generated fragment (Figure 2A, lane 2) has a 3′-hydroxyl and migrates about 0.5 base slower than its corresponding MPE-Fe(II)-generated fragment, which has a 3′-phosphate (Hertzberg & Dervan, 1984). In Figure 2A comparison of lane 1 to lane 2 shows that the *Hin*fI fragment migrates about 1.5 bases slower than the corresponding Maxam–Gilbert fragment (–7 C) which has a lower molecular weight and an extra charge due to a 3′-phosphate (Maxam & Gilbert, 1980). Note that the characteristic profile of the densitometry scans allowed easy alignment of one scan with another. For the noncoding strand of pKCT7P the protected region extends from –17 to –4 while for the coding strand (data not shown) the footprint extends from –16 to –4. Table I summarizes the results of similar experiments that were done on both strands of pRW380 (autoradiograms not shown). Table I also summarizes the protected regions observed in the presence of GTP for both strands of the promoters in pKCT7P and pRW380 (autoradiograms not shown).

Determination of Binding Constants. To determine promoter occupancy, the ratio of percent bound promoters to percent free promoters was calculated by published methods (Galas & Schmitz, 1978; Ikeda & Richardson, 1986). As

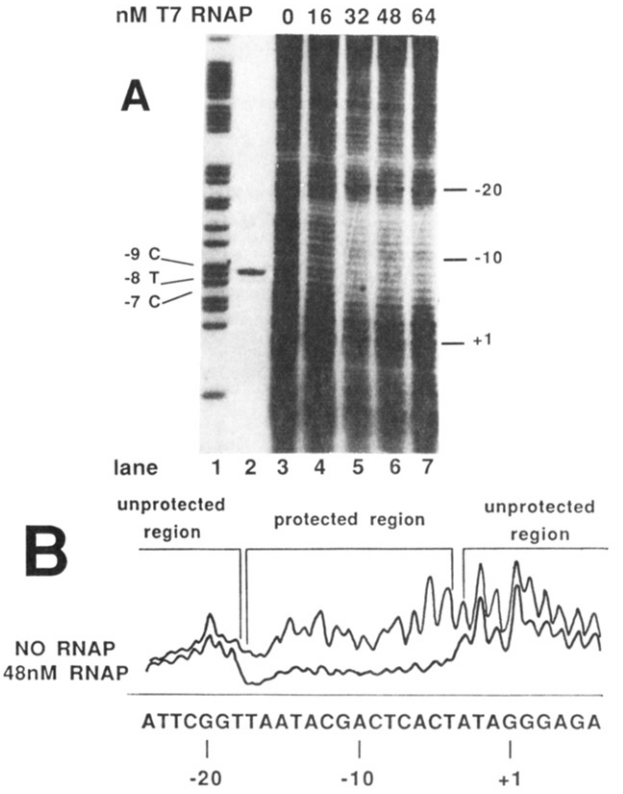

FIGURE 2: Effects of concentration of T7 RNA polymerase on its binding to the promoter from pKCT7P. (A) Autoradiogram of the dependence of T7 RNA polymerase binding to the noncoding strand of the pKCT7P promoter on the concentration of T7 RNA polymerase. For lanes 3–7, standard reaction conditions were used including 2 mM $MgCl_2$, 10 mM NaCl, 6.5% glycerol, and 0.5 nM promoter (3.4 ng). Lanes 3–7 contain the following amounts of T7 RNA polymerase: (lane 3) none, (lane 4) 16 nM (80 ng), (lane 5) 32 nM (160 ng), (lane 6) 48 nM (240 ng), and (lane 7) 64 nM (320 ng). Lane 2 is a *Hin*fI digest of the 205 base pair fragment and corresponds to the –7 position of the promoter. Lane 1 is a G+A Maxam–Gilbert sequencing reaction of the DNA fragment. The positions of the MPE-Fe(II)-generated bands are shown on the right while the positions of the Maxam–Gilbert bands (sequence is of the coding strand) are shown on the left. (B) Densitometric scans of lane 3 (no polymerase) and lane 6 (48 nM polymerase) from the autoradiogram in (A). Both scans are aligned to the promoter sequence (only the coding strand of pKCT7P is shown) by assuming that the *Hin*fI-generated fragment migrates about 0.5 base slower than its corresponding MPE-Fe(II)-generated fragment. Both the protected and unprotected regions are indicated.

Table I: Summary of Protected Regions and Binding Constants for T7 Promoters in the Plasmids pKCT7P and pRW380

	pKCT7P, class II/III hybrid	pRW380, class III
K_{RP} ($\times 10^7$ M^{-1})	4.6 ± 1.4	4 ± 1.5
K_{RP} + GTP ($\times 10^7$ M^{-1})	3.6 ± 1.2	10 ± 1.7
K_{RD} ($\times 10^7$ M^{-1})	(<1.6 ± 1) × 10^{-3}	(<2.1 ± 1.1) × 10^{-3}
protected region		
coding strand	–16 to –4	–19 to –4
noncoding strand	–17 to –4	–20 to –4
protected region (+GTP)		
coding strand	–16 to +6	–19 to +6
noncoding strand	–17 to +5	–20 to +5

shown in Figure 2B, two densitometric scans were aligned, one from the no RNA polymerase reaction (the no RNAP scan) and the other from a reaction containing 48 nM RNA polymerase (the 48 nM RNAP scan). To correct for variations in the counts loaded from each reaction, the entire 48 nM RNAP scan was scaled up or down (normalized) so that the unprotected regions (Figure 2B) of the two scans would match as closely as possible. Normalization was accomplished by

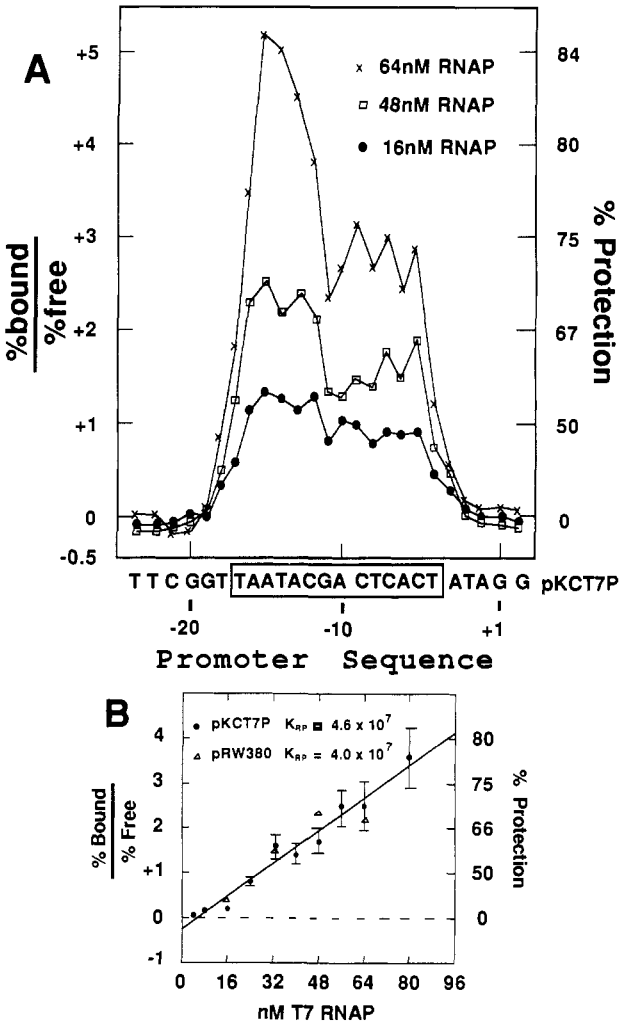

FIGURE 3: Determination of binding constants for promoters in the plasmids pKCT7P and pRW380. (A) The graph is of T7 RNA polymerase occupancy for all bases within and flanking the promoter region of the pKCT7P promoter. Only the sequence of the coding strand is shown. The three curves are three different concentrations of T7 RNA polymerase taken from Figure 2A (see lanes 4, 6, and 7). The formula for determining the ratios of percent bound to percent free for all bases within and flanking the promoter is found in the text. The boxed sequence indicates the protected region. (B) The graph is of RNA polymerase occupancy of the entire promoter site (both pKCT7P and pRW380) vs. concentration of T7 RNA polymerase. The autoradiogram for the pRW380 promoter is not shown. Error bars and the line are indicated only for the pKCT7P promoter. Error bars smaller than ±0.2 unit are not shown. The line is a least-squares fit to the data points (not including the origin).

multiplying all the absorbance values of the 48 nM RNAP scan by the ratio of the unprotected regions between the two scans. For any given base in the sequence (base N), the RNA polymerase occupancy of that base (the ratio of percent bound to percent free for base N) is determined by

$$\frac{\%\text{ bound for base N}}{\%\text{ free for base N}} = \frac{A(\text{base N, no RNAP})}{A^*(\text{base N, 48 nM RNAP})} - 1 \quad (1)$$

A is the absorbance of band N (no polymerase present) on the autoradiogram. A^* is the normalized absorbance of band N in the presence of 48 nM polymerase. A graph of RNA polymerase occupancy for all the base pairs within and flanking the promoter region is shown in Figure 3A (and in Figure 7). An alternative method of determining the amount of DNA in a band is to use the total integrated area under the absorbance peak instead of the absorbance value for band N. However, this substitution did not significantly affect the value of the ratio of percent bound to percent free for base N (data not shown).

Figure 3A shows the curves obtained for three different concentrations of T7 RNA polymerase binding to the noncoding strand of pKCT7P. Note that the curve profile is roughly the same for the different concentrations of polymerase. The most highly protected bases are from −16 to −12, a result confirmed by a similar analysis of the coding strand of the pKCT7P promoter and both strands of the pRW380 promoter (data not shown).

As a consequence of the normalization procedure, the average of the ratio percent bound to percent free values for the entire unprotected region was set equal to 0 with a typical standard deviation of 0.1–0.3. This standard deviation was used for determining the protected bases by the following criteria: a base was considered to be protected if its ratio of percent bound to percent free was greater than 3 standard deviations from 0.

Figure 3B is a graph of the ratio of percent bound to percent free promoter sites vs. concentration of T7 RNA polymerase. Promoter occupancy for the entire RNA polymerase binding site is equal to the average of the ratio of percent bound to percent free for all bases within the protected region. (Examples of promoter occupancy for the entire binding site are shown in Figures 3B, 4B, 5, and 6). The line in the graph is a least-squares fit to the data (origin not included) for only the pKCT7P promoter. With use of published nomenclature, the following derivation demonstrates that the slope of the line is equal to the binding constant K_{RP} for the polymerase–promoter binding reaction (Strauss et al., 1980; Ikeda & Richardson, 1986):

$$K_{RP} = \frac{[RP]}{[R]_f[P]_f} = \frac{\%\text{ bound promoter}}{[R]_f(\%\text{ free promoter})} \quad (2)$$

with

$$[R]_T = [R]_f + [RP] + [RD] \quad (3)$$

[RP] is the concentration of the polymerase–promoter complex, $[P]_f$ is the free promoter concentration, $[R]_f$ is the free polymerase concentration, $[R]_T$ is the total polymerase concentration, and [RD] is the concentration of polymerase–nonspecific DNA complexes. In eq 2, the ratio of [RP] to $[P]_f$ is equal to the ratio of percent bound to percent free promoters for the entire promoter site. In eq 3, $[RP] \ll [R]_T$ because the polymerase is in molar excess (minimally 32:1) of the promoter. We also observed that $[RD] \ll [R]_T$ because different size promoter-bearing DNA fragments (144 base pairs vs. 317 base pairs) yielded identical values of K_{RP}. This observation was verified by noting that the presence of 100 ng of nonpromoter-bearing DNA (50-fold excess in molar base pairs over the DNA probe) had no significant affect on K_{RP} (see Figure 6). Thus, eq 3 reduces to $[R]_T = [R]_f$, which was substituted into eq 2 to give

$$K_{RP} = \frac{\%\text{ bound promoter}}{[R]_T(\%\text{ free promoter})} \quad (4)$$

Figure 3B is a graph of the ratio of percent bound to percent free promoters vs. total RNA polymerase concentration. Utilizing eq 4, this plot gives a line with a slope equal to K_{RP}. The binding constant for the pKCT7P promoter is (4.6 ± 1.4) × 10^7 M^{-1} and for the pRW380 promoter is (4 ± 1.5) × 10^7 M^{-1} (autoradiogram not shown for pRW380). The difference between the two binding constants is not significant. However, Table I indicates that in the presence of GTP the binding

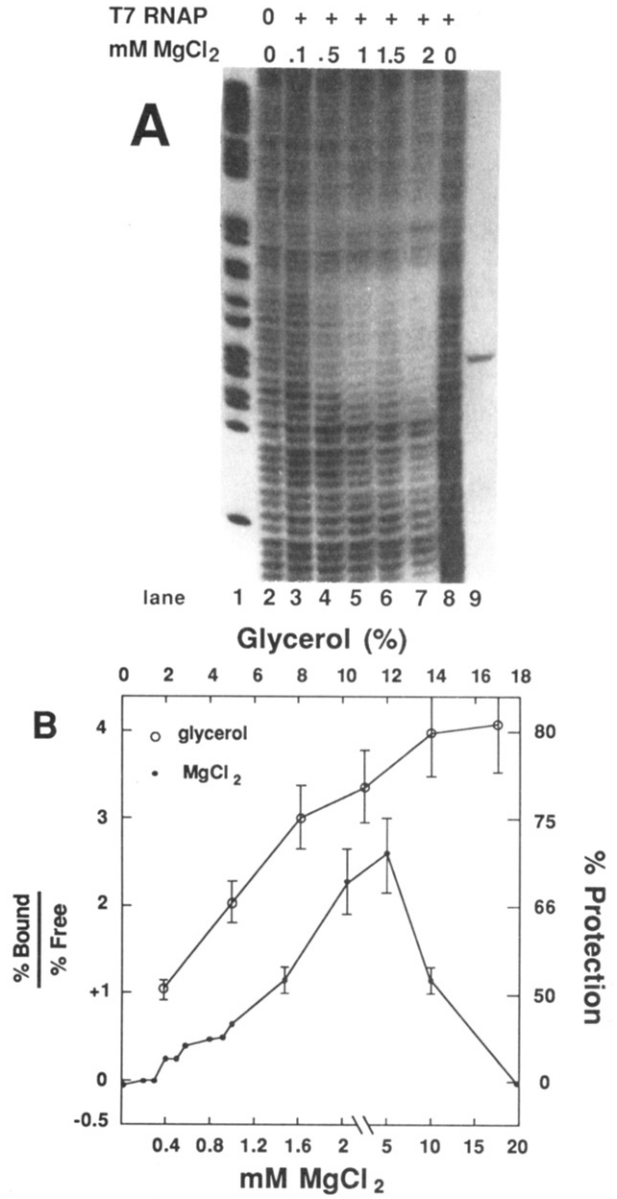

FIGURE 4: Effects of $MgCl_2$ and glycerol on T7 RNA polymerase binding. (A) The autoradiogram shows the dependence of the binding reaction on $MgCl_2$. Standard reaction conditions were used including 3.3% glycerol, no NaCl, and 0.5 nM (3.4 ng) of the 205 base pair fragment of the noncoding strand of the pKCT7P promoter. Lane 2 has no polymerase while lanes 3–8 have 80 nM T7 RNA polymerase. Lanes 2–8 contain the following concentrations of $MgCl_2$: (lanes 2 and 8) none, (lane 3) 0.1 mM, (lane 4) 0.5 mM, (lane 5) 1 mM, (lane 6) 1.5 mM, and (lane 7) 2 mM. Lane 9 is the full-length fragment digested with *Hin*fI, which generates a band at the −7 position. Lane 1 is a Maxam–Gilbert G reaction of the full-length fragment. (B) Graph of promoter occupancy vs. $MgCl_2$ (lower axis) and glycerol (upper axis). Analysis of the densitometry of the autoradiogram in (A) is explained in Figures 2B and 3B. The autoradiogram of the effects of glycerol on binding is not shown. The ordinate is the ratio of percent bound to percent free determined for the entire polymerase binding site as described in Figures 3B and in the text. The data for 5, 10, and 20 mM $MgCl_2$ was taken from other autoradiograms. Error bars smaller than ±0.2 (in units of percent bound to percent free promoters) are not shown.

constant of the pRW380 promoter is 3 times greater than that for the pKCT7P promoter (autoradiograms are not shown).

Effects of $MgCl_2$ and Glycerol on Binding of T7 RNA Polymerase to the pKCT7P Promoter. The autoradiogram in Figure 4A shows the $MgCl_2$ effects on the binding of T7 RNA polymerase to the noncoding strand of the pKCT7P promoter. Reaction conditions were standard except 3.3% glycerol was used in the reaction and NaCl was omitted. Specific reaction conditions are given in the figure legend. Figure 4B is a graph of the ratio of percent bound to percent free promoter sites vs. the concentration of $MgCl_2$ (lower axis) or glycerol percentage (upper axis). The graph shows that from 0 to 20 mM $MgCl_2$ (lower axis) the number of promoters bound by the polymerase increases until it peaks from 2 to 5 mM $MgCl_2$. From 5 to 20 mM $MgCl_2$ the number of promoters bound by the polymerase decreases to 0. Thus under our conditions the optimal $MgCl_2$ range for binding is from 2 to 5 mM with no binding seen at either 0 or 20 mM. Note that similar results were obtained when the coding strand of pKCT7P was analyzed (data not shown).

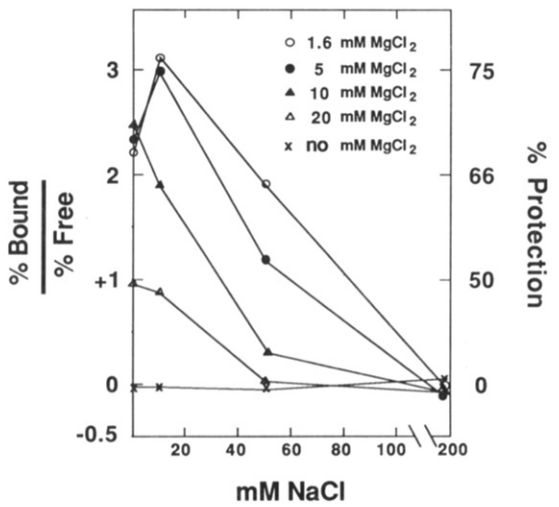

FIGURE 5: Graph of dependence of T7 RNA polymerase binding on NaCl and $MgCl_2$. The autoradiogram is not shown, but standard reaction conditions were used including 80 nM T7 RNA polymerase, 3.3% glycerol, and 0.4 nM of the 205 base pair fragment from the pKCT7P promoter. The ordinate is the ratio of percent bound to percent free determined for the entire polymerase binding site as described in Figure 3B and in the text. Note that four concentrations of NaCl were assayed: 0, 10, 50, and 200 mM NaCl. Each concentration of NaCl was assayed at five different concentrations of $MgCl_2$: 0, 1.6, 5, 10, and 20 mM $MgCl_2$.

Figure 4B also graphs the dependence of the binding reaction on glycerol (upper axis). The autoradiogram of glycerol dependence is not shown. The specific reaction conditions were 2 mM $MgCl_2$, 10 mM NaCl, 48 nM T7 RNA polymerase, and 0.5 nM coding strand of the pKCT7P promoter. A similar curve was generated when the noncoding strand of pKCT7P was analyzed (data not shown). To decrease the possibility that glycerol is merely stabilizing or preventing polymerase degradation, a variety of dilutions and times after dilution of T7 RNA polymerase were used. All of these experiments gave results similar to the glycerol curve in Figure 4B (data not shown).

Effects of both $MgCl_2$ and NaCl on Binding of T7 RNA Polymerase to the pKCT7P Promoter. The graph in Figure 5 shows the effect of $MgCl_2$ and NaCl on the binding reaction. The optimal ionic conditions for binding are from 0 to 10 mM NaCl and from 2 to 5 mM $MgCl_2$. Regardless of the $MgCl_2$ concentration, 200 mM NaCl completely inhibited the binding. The no $MgCl_2$ curve also shows no binding at any concentration of NaCl; this implies the Mg^{2+} ion is absolutely required for T7 RNA polymerase to bind to the late promoters. Bacterial polymerase–promoter interactions do not have corresponding requirement for Mg^{2+}. Footprints were obtained when the Mg^{2+} cation was replaced by either Ca^{2+}, Mn^{2+}, or magnesium glutamate at concentrations of 1, 3, or 10 mM (data not shown). However, no footprints were observed if

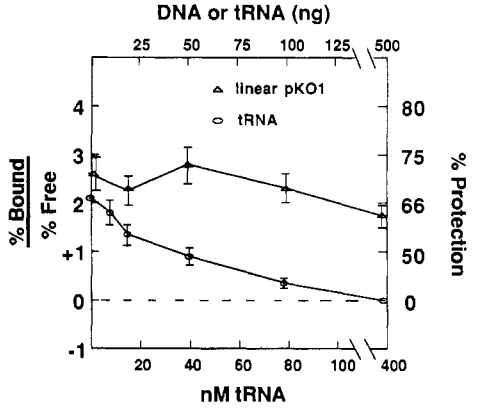

FIGURE 6: Effects of both tRNA and nonpromoter-bearing DNA on T7 RNA polymerase binding. Graph of promoter occupancy vs. tRNA and pKO1. The autoradiogram is not shown, but standard reaction conditions were used including 2 mM $MgCl_2$, 10 mM NaCl, 5% glycerol, and 0.5 nM (3.4 ng) of the 205 base pair fragment of the noncoding strand of the pKCT7P promoter. The ordinate is the ratio of percent bound to percent free for the entire polymerase binding site as described in Figure 3B and in the text. The upper axis is in nanograms of tRNA or pK01 added to the reaction while the lower axis is nanomolar tRNA. Yeast tRNA was obtained from Sigma and was further purified as described under Materials and Methods.

$MgCl_2$ was replaced with either potassium glutamate, sodium glutamate, sodium chloride, spermidine, putrescine, or glutamic acid (pH 7.4) at concentrations of 1, 3, or 10 mM (data not shown).

Effects of tRNA and Nonpromoter-Bearing DNA on Binding of T7 RNA Polymerase to the pKCT7P Promoter. The graph in Figure 6 shows the effect of tRNA or pKO1 on the binding reaction. pKO1, the parent plasmid of pKCT7P, contains no T7 promoters. pKO1 was linearized with *Bam*H1 before addition to the reaction. (Note that both tRNA and pKO1 were present along with the labeled DNA before the addition of the polymerase.) The graph shows that tRNA stoichiometrically inhibits T7 RNA polymerase from binding to the T7 promoter. However, equimolar base pairs of pKO1 (upper axis) inhibit the binding only slightly. Other nonpromoter-bearing DNAs such as λ (cut with *Hin*dIII), pBR322, and *E. coli* K12 also cause only a slight inhibition of the binding (data not shown).

Further experiments suggest that an upper limit can be determined for a nonspecific binding constant, K_{RD}, for T7 RNA polymerase binding to nonspecific DNA sites. Using nomenclature from eq 1–4 and using [D] as the concentration of nonspecific promoter sites (Strauss et al., 1980), the formula for K_{RD} is

$$K_{RD} = \frac{[RD]}{[R]_f[D]} \quad (5)$$

where

$$[D] = 2[\text{base pairs}] \quad (6)$$

However, $[RP] \ll [R]_T$; therefore, eq 3 becomes

$$[RD] = [R]_T - [R]_f \quad (7)$$

Substituting eq 6 and 7 into eq 5 and rearranging yields

$$2K_{RD}[\text{base pairs}] + 1 = [R]_T/[R]_f \quad (8)$$

Plotting $[R]_T/[R]_f$ vs. 2 [base pairs] would yield a line with a slope equal to K_{RD}. The values for [base pairs] and $[R]_T$ are known. By use of a labeled fragment from either pKCT7P or pRW380 and the value of K_{RP} corresponding to that

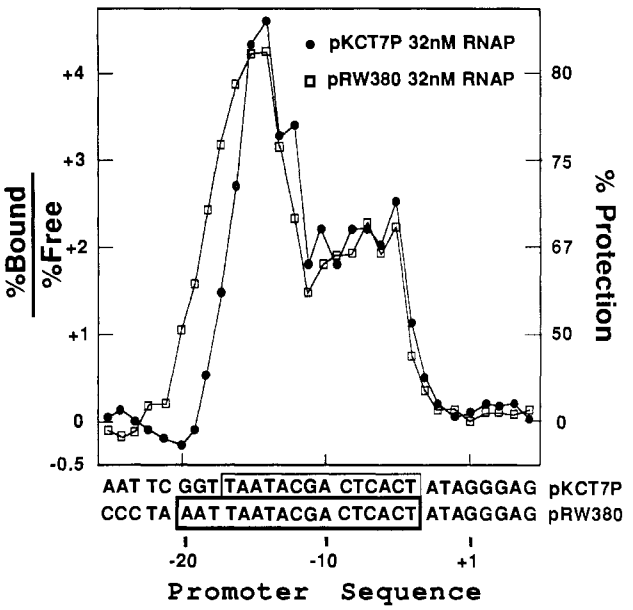

FIGURE 7: Difference in size of the protected region between the promoters from pKCT7P and pRW380. The graph is of the RNA polymerase occupancy for all the bases within and flanking the promoter region for the noncoding strands of pKCT7P and pRW380. Only the coding strand of both promoters is shown. Standard reaction conditions were used including 32 nM T7 RNA polymerase, 2 mM $MgCl_2$, 10 mM NaCl, and 6.5% glycerol. The protected region is boxed for pKCT7P and boxed with a heavier line for pRW380.

fragment, $[R]_f$ can be determined from eq 2. [Note: although K_{RP} was determined by assuming [RD] is negligible (see eq 4), eq 2 makes no assumptions on the value of [RD]. Therefore, eq 2 may be used for determining $[R]_f$.] *Nru*1-linearized pKO1 (one cleavage site in the plasmid) was used as the nonspecific DNA. To ensure end binding was not significantly reducing the $[R]_f$ value, parallel experiments were performed with *Sau*3A-digested pKO1 (21 cleavage sites in the plasmid). At 37 °C, 2 mM $MgCl_2$, 10 mM NaCl, 0.5 nM of the 317 base pair coding strand of pRW380, and 100 nM T7 RNA polymerase, the value of K_{RD} for *Nru*1-digested pKO1 was determined to be $(2.1 \pm 1.2) \times 10^4$ M^{-1} (data not shown). The value of K_{RD} between *Nru*1- and *Sau*3A-digested pKO1 did not differ significantly, implying that end binding was not causing the reduction in $[R]_f$. [Note that a similar value of K_{RD} was obtained when the labeled promoter was from pKCT7P (see Table I).] The equilibrium selectivity ratio (ESR) is the ratio of K_{RP} to K_{RD} (Strauss et al., 1980); therefore, the ESR value of T7 RNA polymerase under these low ionic conditions is approximately 2000.

Comparison of the Protected Sequences between the Promoters from pKCT7P and pRW380. Figure 7 is a graph of the ratio of percent bound to percent free for all the bases within and flanking the promoters from pKCT7P and pRW380. A description of this method of analysis is found in Figure 3A and in the text. The footprint reactions of both promoters were done under identical conditions and on the same polyacrylamide gel. Also, the autoradiographs were scanned under identical conditions. In Figure 7 the protection curves of both promoters overlap within the −15 to +5 region. However, in the −25 to −16 region the two curves do not overlap. Instead, the pRW380 curve indicates the polymerase is protecting three extra bases (−20 to −18) at the 5′ end of the promoter. This extra protection was seen for four other concentrations of polymerase analyzed and also when the coding strands of both promoters were compared (see Table I). Table I also indicates that in the presence of GTP the same

three bases were still protected only in the pRW380 promoter.

Discussion

This paper investigates the interactions of T7 RNA polymerase with T7 late promoters by MPE-Fe(II) footprinting. Footprints were obtained at concentrations of T7 RNA polymerase roughly 50–400 times lower than that previously reported (Ikeda & Richardson, 1986). This resulted in a binding constant for a class III promoter of $(4 \pm 1.5) \times 10^7$ M^{-1} and in the presence of GTP of $(10 \pm 1.7) \times 10^7$ M^{-1}. These two binding constants are 1000 and 200 times greater, respectively, than those previously reported (Ikeda & Richardson, 1986). Table I summarizes the values of K_{RP}, K_{RP} in the presence of GTP and K_{RD} for the promoters from the plasmids pKCT7P and pRW380. Also summarized are the regions protected from MPE-Fe(II) cleavage for both strands of the two promoters both in the presence and in the absence of GTP. Note that the boundaries of protection for pRW380 (±GTP) agree closely with a previous report (Ikeda & Richardson, 1986).

The footprinting reaction conditions were varied to optimize the binding of T7 RNA polymerae to T7 late promoters. As shown in Figures 4 and 5, the optimal ionic conditions for binding are 2–5 mM $MgCl_2$ and 0–10 mM NaCl. These conditions agree closely with that needed for optimal in vitro transcription activity (unpublished results). Surprisingly, Mg^{2+} was necessary to obtain binding. Neither spermidine, putrescine, potassium glutamate, sodium glutamate, sodium chloride, or glutamic acid could substitute for Mg^{2+}; however, magnesium glutamate, Ca^{2+}, or Mn^{2+} could substitute for Mg^{2+} to give a footprint.

Several explanations may account for the dependence of polymerase–promoter complex formation on the presence of the Mg^{2+} cation. (1) The ESR value of T7 RNA polymerase may increase in the presence of the Mg^{2+} cation. At low or no Mg^{2+} concentration, most of the polymerase could be bound to nonspecific promoter sites, thus lowering the free polymerase concentration. From 0 to 2 mM $MgCl_2$, the ESR value increases, which releases the nonspecifically bound polymerase. Similar ionic effects on ESR are observed for *E. coli* holoenzyme (Strauss et al., 1980). (2) Mg^{2+} might stabilize a promoter or polymerase conformation favorable for binding. (3) Although the binding constant of MPE-Fe(II) to DNA is about 1×10^5 M^{-1} (Hertzberg & Dervan, 1984), only one MPE-Fe(II) molecule bound to the promoter site is sufficient to displace the polymerase. If we assume that Mg^{2+} dramatically decreases the binding affinity of MPE-Fe(II) to DNA, then polymerase binding would be favored. However, large variations in either NaCl (±0.5 M) or $MgCl_2$ (±20 mM) have little effect on the binding constant of MPE-Fe(II) to DNA (Hertzberg & Dervan, 1984). Also ethidium bromide (an intercalative analogue of MPE) does not exhibit dramatic changes in affinity for DNA under a variety of ionic conditions (Bresloff & Crothers, 1981; Kastrup et al., 1978). Therefore, the third explanation can probably be ignored.

From 5 to 20 mM $MgCl_2$ and from 10 to 200 mM NaCl, ionic effects appear to dominate the binding reaction. Other investigators have postulated that the Mg^{2+} cation (and to a lesser extent the Na^+ cation) inhibits the protein–DNA interactions by competing for phosphates on the DNA backbone (Record et al., 1977; Strauss et al., 1980). Our results partly support this idea. Although Mg^{2+} is required for binding to occur, concentrations of $Mg^{2+} > 5$ mM inhibit the binding reaction. Concentrations of NaCl > 10 mM also inhibit the binding reaction.

The graph in Figure 4B (upper axis only) indicates that the binding reaction was stabilized by glycerol. In contrast, in vitro transcription assays indicate that increasing glycerol reduces the activity of T7 RNA polymerase (unpublished results). However, the possibility that glycerol enhances the binding reaction by preventing inactivation of T7 RNA polymerase cannot be ruled out.

We also found that tRNA stoichiometrically inhibits T7 RNA polymerase from binding to T7 late promoters. Equimolar base pairs of nonpromoter-bearing DNA do not inhibit binding, suggesting that the nucleotide concentration of tRNA is not the cause of inhibition. Because nonpromoter-bearing DNA (pKO1) does not significantly inhibit the binding reaction, an estimate on the nonspecific binding constant, K_{RD}, was calculated to be $(2.1 \pm 1.1) \times 10^4$ M^{-1}. Several factors that might effect the value of K_{RD} are as follows: (1) end binding (and perhaps nick binding) cannot be ruled out, (2) the T7 RNA polymerase preparation may not be 100% active, and (3) the addition of nonspecific DNA may be adding undesired $MgCl_2$ and/or NaCl to the reaction, thereby lowering the percent bound to percent free ratio of the highly salt-sensitive complex (see Figure 5). With this value of K_{RD}, an estimate of 2000 can be set on the ESR value of T7 RNA polymerase. In contrast, ESR values for *E. coli* holoenzyme range from 5000 to 80 000 (at 37 °C) (Strauss et al., 1980). However, any comparison of the ESR and K_{RD} values between T7 and *E. coli* RNA polymerase is probably invalid because these values have not been measured under identical ionic conditions.

In the presence of GTP we found that the protected region extends from −20 to +5 for the pRW380 promoter. Thus, the polymerase is binding the entire consensus region (or at least melting the DNA), leaving no conserved sequences open for the binding of any putative regulatory proteins.

The three extra bases of protection (see Table I) between the promoters from the plasmids pKCT7P and pRW380 are interesting because both promoters show identical binding constants (in the absence of GTP). This implies that the −20 to −17 region (both strands) is not contributing to the thermodynamic stability of the polymerase–promoter interaction. However, in the presence of GTP, the binding constant of the pRW380 promoter is 3 times that of the pKCT7P promoter. Thus, the −20 to −18 region appears to be necessary to stabilize the promoter–polymerase complex in the presence of GTP. Finally, this region has been implicated in determining the salt dependencies of promoter activity as seen by in vitro transcription studies (Jollife et al., 1982). Promoters with a class II −22 to −18 region are more salt sensitive than promoters with a class III −22 to −18 region. Experiments are under way to compare the in vitro salt sensitivities of the binding constants of pRW380 and pKCT7P.

Acknowledgments

We thank the research group of Dr. Tom Record for suggestions and criticisms, and we are grateful to Greg Bellamy and Jim Murphy for critically reviewing the manuscript. We are also indebted to Jim Hu for assistance in the computer analysis of the densitometry, Dr. Peter B. Dervan for providing us with MPE, Dr. F. W. Studier for providing us with a T7 RNA polymerase overproducing strain, and Dr. R. A. Ikeda for sending us his research results prior to publication.

References

Basu, S., & Maitra, U. (1986) *J. Mol. Biol. 190*, 425–437.

Bresloff, J. L., & Crothers, D. M. (1981) *Biochemistry 20*, 3547–3553.

Burgess, R. R. (1969) *J. Biol. Chem. 244*, 6168–6176.

Chamberlin, M., McGrath, J., & Waskell, L. (1970) *Nature (London) 228*, 227–231.
Chapman, K. A., & Wells, R. D. (1982) *Nucleic Acids Res. 10*, 6331–6340.
Davanloo, P., Rosenberg, A. H., Dunn, J. J., & Studier, F. W. (1984) *Proc. Natl. Acad. Sci. U.S.A. 81*, 2035–2039.
Dunn, J. J., & Studier, F. W. (1983) *J. Mol. Biol. 166*, 477–535.
Galas, D. J., & Schmitz, A. (1978) *Nucleic Acids Res. 5*, 3157–3170.
Hertzberg, R. P., & Dervan, P. B. (1982) *J. Am. Chem. Soc. 104*, 313–315.
Hertzberg, R. P., & Dervan, P. B. (1984) *Biochemistry 23*, 3934–3945.
Ikeda, R. A., & Richardson, C. C. (1986) *Proc. Natl. Acad. Sci. U.S.A. 83*, 3614–3618.
Jollife, L. K., Carter, A. D., & McAllister, W. T. (1982) *Nature (London) 299*, 653–656.
Kastrup, R. V., Young, M. A., & Krugh, T. R. (1978) *Biochemistry 17*, 4855–4865.
Kornberg, A. (1980) in *DNA Replication*, pp 139–142, Freeman, San Francisco.
Maxam, A. M., & Gilbert, W. (1980) *Methods Enzymol. 65*, 520–523.
McAllister, W. T., Morris, C., Rosenberg, A. H., & Studier, F. W. (1981) *J. Mol. Biol. 153*, 527–544.
Record, M. T., deHaseth, P. L., & Lohman, T. M. (1977) *Biochemistry 16*, 4791–4796.
Schneider, T. D., Stormo, G. D., Gold, L., & Ehrenfeucht, A. (1986) *J. Mol. Biol. 188*, 415–431.
Strauss, H. S., Burgess, R. R., & Record, M. T. (1980) *Biochemistry 19*, 3504–3515.
Studier, F. W., & Rosenberg, A. H. (1981) *J. Mol. Biol. 153*, 503–525.
Tabor, S., & Richardson, C. C. (1985) *Proc. Natl. Acad. Sci. U.S.A. 82*, 1074–1078.

Fluorescence Photobleaching Analysis of Nuclear Transport: Dynamic Evidence for Auxiliary Channels in Detergent-Treated Nuclei†

Lian-Wei Jiang‡ and Melvin Schindler*
Department of Biochemistry, Michigan State University, East Lansing, Michigan 48824
Received April 29, 1986; Revised Manuscript Received October 28, 1986

ABSTRACT: Nuclear transport experiments were performed on isolated rat liver nuclei to examine the permeability of membrane and detergent-free peripheral nuclear lamina. The transport of 64K molecular weight fluorescent-derivatized dextrans was measured by using the technique of fluorescence redistribution after photobleaching. Results of these experiments provide evidence for transport pathways that appear to be functionally distinct from nuclear pore complex channels. The suggestion is made that these supplemental pathways are embedded in the peripheral nuclear lamina and are normally masked by the inner nuclear membrane.

Nucleocytoplasmic communication appears to be mediated by a multicomponent octagonally symmetric cylindrical structure spanning the double membrane of the nucleus (deRobertis, 1983; Gall, 1967; Kessel, 1973). These nuclear pore complexes have been investigated by a number of microscopic techniques which, for the most part, suggest a hollow cylinder containing strandlike structures. The cytoplasmic face of the nuclear pore complex is decorated with spherical components (Kessel, 1973; Unwin & Milligan, 1982). In all cases, these pore complexes have been visualized in nuclei that have retained their membranes following isolation (Kessel, 1973; Unwin & Milligan, 1982) or nuclei that have been treated with the detergent Triton X-100 (Kirschner et al., 1977; Schindler, 1984). Recently, Schindler and Hogan (1985) succeeded in preparing nuclei that had neither membranes nor detergent bound to their surfaces. In addition, the content of lamins (A, B, and C) was significantly reduced. The exposed nuclear surface showed a highly pebbled surface consisting of an interlocking array of circular particles with diameters of ~80–100 nm. Many of these particles had holes in their center and suggested the structure of pore complexes without the octagonal bonnet of annular subunits. Such structures have also been observed by Kuzmina et al. (1981), Schatten and Thoman (1978), and Kirschner et al. (1977), who considered them incomplete pore complexes. The surface density of these structures was 2–3 times that observed for "classic" pore complexes in whole nuclei or nuclei following Triton X-100 treatment (Kirschner et al., 1977). The suggestion was made that such structures may serve as preformed pore templates capable of activation to form complete nuclear pore complexes (Schindler & Hogan, 1985). This was an appealing hypothesis considering the dynamic nature of pore assembly and disassembly which appears to vary with cell metabolism and stimulation (Maul, 1977a,b). The pore precursor suggestion also correlated with observations that pore synthesis was found to occur without concomitant protein biosynthesis (Maul, 1977a,b) or nuclear surface expansion (Maul & Deaven, 1977). To investigate the possibility that the holes observed in detergent and membrane-free nuclei may indeed serve as potential transport routes, we have examined the transport rate of 64K molecular weight fluorescent-labeled dextrans into nuclei treated with a number of membrane-active agents. Using the technique of fluorescence redistribution after photobleaching (FRAP), we observe transport rates that suggest the holes, observed following detergent treatment, have some of the transport properties of nuclear pore complexes as previously demonstrated by Jiang and Schindler (1986), Schindler and Jiang (1986), and Peters (1983, 1984).

† This work was supported by NIH Grant GM 30158.
‡ Permanent address: Department of Medical Physics, Beijing Medical University, Beijing, China.

0006-2960/87/0426-1546$01.50/0